

No evidence for gamma-ray halos around active galactic nuclei resulting from intergalactic magnetic fields (Research Note)

A. Neronov^{1,2}, D. V. Semikoz^{3,4}, P. G. Tinyakov^{4,5}, and I. I. Tkachev⁴

¹ ISDC Data Centre for Astrophysics, Ch. d'Ecogia 16, 1290 Versoix, Switzerland
e-mail: andrii.neronov@unige.ch

² Geneva Observatory, Ch. des Maillettes 51, 1290 Sauverny, Switzerland

³ APC, 10 rue Alice Domon et Leonie Duquet, 75205 Paris Cedex 13, France

⁴ Institute for Nuclear Research RAS, 60th October Anniversary prosp. 7a, Moscow 117312, Russia

⁵ Service de Physique Theorique, Universite Libre de Bruxelles, CP225, blv. du Triomphe, 1050 Bruxelles, Belgium

Received 8 October 2010 / Accepted 18 November 2010

ABSTRACT

We analyze the gamma-ray halo around stacked AGNs reported by Ando & Kusenko (2010, ApJ, 722, L39). First, we show that the angular distribution of γ -rays around the stacked AGNs is consistent with the angular distribution of the γ -rays around the Crab pulsar, which is a point source for *Fermi*/LAT. This makes it unlikely that the halo is caused by an electromagnetic cascade of TeV photons in the intergalactic space. We then compare the angular distribution of γ -rays around the stacked AGNs with the point-spread function (PSF) of *Fermi*/LAT and confirm the existence of an excess above the PSF. However, we demonstrate that the magnitude and the angular size of this effect is different for photons converted in the front and back parts of the *Fermi*/LAT instrument, and thus is an instrumental effect.

Key words. magnetic fields – galaxies: active – gamma rays: galaxies

High-energy gamma rays propagating through the Universe produce electron-positron pairs in interactions with the extragalactic background light (Kneiske et al. 2004; Franceschini et al. 2008; Stecker & Scully 2009). The leading particle of the pair then upscatters the background photons through the inverse Compton effect, creating an electromagnetic cascade. If there is a weak intergalactic magnetic field, electrons and positrons in the cascade are deflected from the original direction before being converted back to photons. These secondary photons create a “halo” of softer gamma-ray photons around an extragalactic TeV gamma-ray source (Aharonian et al. 1994; Plaga 1995; Neronov & Semikoz 2007; Takahashi et al. 2008; Elyiv et al. 2009; Dolag et al. 2009; Neronov et al. 2010). This process may be used to constrain the parameters of the extragalactic magnetic fields (Plaga 1995; Neronov & Semikoz 2007; Takahashi et al. 2008; Elyiv et al. 2009). The absorption of TeV γ -rays leads to the cascade emission in the GeV energy range, which is accessible for observations with the *Fermi* telescope (Neronov & Semikoz 2009). Non-detection of extended emission around blazars with hard intrinsic spectra extending to the multi-TeV energy range by *Fermi* was used to derive a lower boundary on magnetic fields in the intergalactic medium at the level of 10^{-17} G to 10^{-15} G, depending on the assumptions about the intrinsic spectral properties of the analyzed sources (Neronov & Vovk 2010; Tavecchio et al. 2010a,b; Dolag et al. 2011).

Ando & Kusenko (2010) recently claimed to possess evidence for the gamma-ray halos around AGNs from the *Fermi* source catalog. The halo was found in the stacked signal of AGNs selected by certain criteria. It was interpreted to be caused by cascading and deflections of TeV photons in the extragalactic

magnetic fields. Unfortunately, we find that the proposed interpretation of the halo is unlikely, but a more probable cause is a tail in the point-spread function (PSF) of photons pair converted in the back thick layer of the *Fermi* detector.

Our argument consists of two parts.

First, we compare the stacked AGN signal to the signal of the Crab pulsar. This is a bright galactic gamma-ray source whose signal in the *Fermi* energy band consists of two contributions: emission from the pulsar and from the associated pulsar wind nebula (PWN). The Crab PWN has an angular size $\approx 0.05^\circ$ (Hester 2008), which is below the angular resolution of the LAT telescope onboard *Fermi*. This means that the Crab PWN is a point source for LAT. In addition, this PWN is situated in the Galactic anti-center region, where the density of sources in the multi-GeV energy band is low and the diffuse Galactic γ -ray background is relatively low as well. This means that Crab signal is not contaminated by the nearby point sources or by strong inhomogeneities of the diffuse background, and the source can be considered as an isolated point source.

The LAT PSF depends on the photon energy. Thus, the shape of the angular distribution of γ -rays around a source depends on the source spectrum. The total Crab pulsar+PWN spectrum in the 10–100 GeV band is well described by a power law $dN/dE \sim E^{-\Gamma}$ with the photon index $\Gamma \approx 2$ (Abdo et al. 2010), which is the same as the cumulative spectrum of the AGNs derived by Ando & Kusenko (2010). This implies that the point-source contribution to the AGN signal should have the same angular shape as the Crab signal. Thus, a difference between the angular distributions of photons around AGN and the Crab PWN

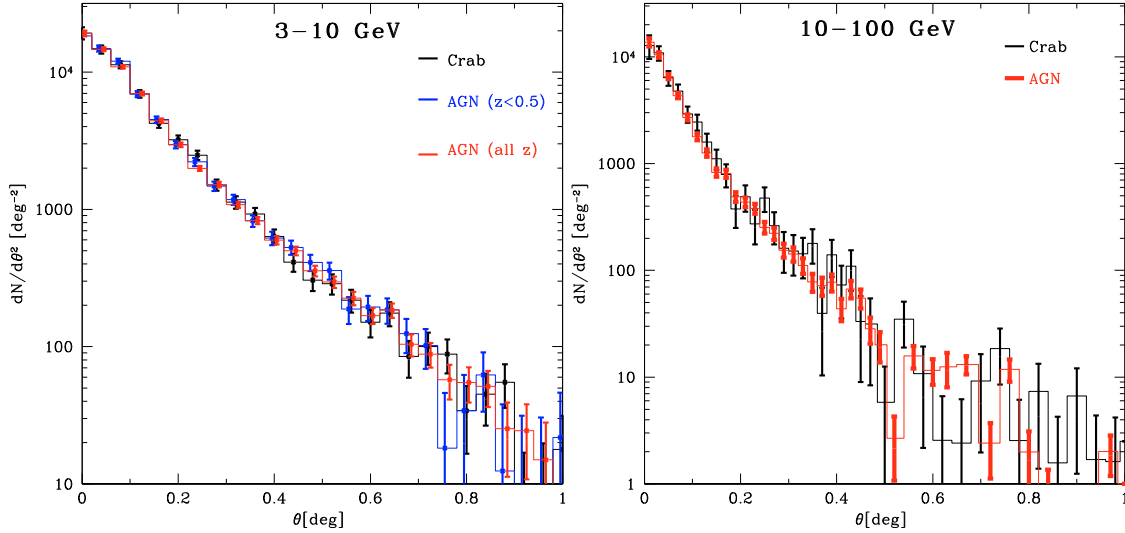


Fig. 1. Comparison of the background-subtracted angular distributions of 3–10 GeV (*left*) 10–100 GeV (*right*) γ -rays around the position of the Crab pulsar (black) and around the stacked AGNs (red). Normalization of the distribution of γ -rays around AGN is scaled to match the γ -ray distribution around the Crab pulsar. In the 3–10 GeV band AGN with redshift $z < 0.5$ are shown in blue.

would indicate a halo around AGNs in addition to the point-source contribution.

Figure 1 shows the angular distribution of photons around the stacked AGNs (red) and the Crab source (black). In both cases the background is subtracted. The shapes of the two signals coincide, which means that the entire stacked AGN signal is well described by a point-source signal, with no additional halo contribution. In an update of their analysis, Ando & Kusenko (2010) have claimed that the halo signal appears only in a subset of AGN at low redshift, $z < 0.5$ and only in the 3–10 GeV energy band. To allow an explicit comparison with Fig. 4 of Ando & Kusenko (2010), we show in blue the photon distribution around AGN at $z < 0.5$ in the left panel of Fig. 1, which corresponds to photon distributions in the 3–10 GeV band. No discrepancy between the Crab PWN and AGN profiles is seen in this case either.

Second, we have investigated the nature of the excess in the angular distribution of photons around AGN above the LAT PSF in the energy range 10–100 GeV. γ -rays detected by the LAT telescope are split into two types: photons that are pair-converted in the thin front layer of the LAT detector (“front” photons), and photons converted in the thick back layer (“back” photons) (Abdo et al. 2009). The shapes of the PSF for these two types of photons are significantly different. Taking this into account, we split the entire photon signal from the set of AGNs considered by Ando & Kusenko (2010) into two parts corresponding to the front and back converted photons and analyze each part separately. We then compare the angular distributions of the front and back photons with the corresponding PSFs calculated using the DIFFUSE_P6_v3 calibration files by averaging the PSF for a given photon energy and incidence angle over the entire set of energies and incidence angles of detected photons from the AGN set.

The angular distribution of all (front + back) photons around AGN is shown in Fig. 2 together with the corresponding PSF. We find an excess in the data at $0.2^\circ < \theta < 0.9^\circ$ for the 10–100 GeV band and in the 0.5° – 1° range in 3–10 GeV band. There is a significant difference between our estimate of the background level shown in Fig. 2 and the background level in the Fig. 2 of Ando & Kusenko (2010), which is a factor of ≈ 3 higher than

our estimate in the 10–100 GeV band. The constant background level shown in Fig. 2 was derived from fitting of the data in the range $0 < \theta < 2^\circ$ around AGN with a model consisting of PSF plus a constant.

We have checked that our estimate of the background level is self-consistent in the following way. The total number of photons detected by *Fermi* in the energy band 10–100 GeV in the Galactic latitude range $|b| > 10^\circ$ is $N_{\text{total}} \approx 5.6 \times 10^4$. Only a small fraction of these photons, $N_{\text{source}} \approx 0.6 \times 10^4$ could be associated to the known *Fermi* sources. The remaining photons contribute to the diffuse Galactic and extragalactic backgrounds. Dividing the number of diffuse background photons by the solid angle Ω spanned by the considered part of the sky, one finds the surface brightness of the background $dN/d\theta^2 \approx (N_{\text{total}} - N_{\text{source}})/\Omega \approx 1.5 \text{ deg}^{-2}$. Multiplying this number by the number of AGN considered in the analysis one arrives at the background estimate consistent with the one shown in Fig. 2. We stress that this background estimate is significantly lower than that found by Ando & Kusenko (2010)

The angular distributions of front and back photons separately are shown in Fig. 3, each with the corresponding PSF. One can see that the front photons have more compact PSF, which is reasonably compatible with the angular distribution of the front photon part of the AGN signal. The fit of the data in the range $0 < \theta < 2^\circ$ by the PSF + background gives $\chi^2/\text{d.o.f.} = 125/98$ ($p \sim 3\%$) in the 10–100 GeV band. Top panels of Fig. 3 show the angular distributions of front and back photons in the 3–10 GeV band. Obviously there is no hint of excess above the PSF of the front photons in this energy band. The reduced χ^2 of the fit is $\chi^2/\text{d.o.f.} = 67/72$.

The back photons have a wider PSF, which does not reproduce the back part of the AGN signal in either 3–10 GeV or 10–100 GeV energy range.

Adding front and back photon signals one can verify that most of the excess above the DIFFUSE_P6_v3 PSF in Fig. 2 is caused by the back photons. There is no strong excess above the PSF in the front photon signal. This indicates that the excess of the photons above the PSF, reported in Ando & Kusenko (2010), cannot be attributed to the extended emission around AGN,

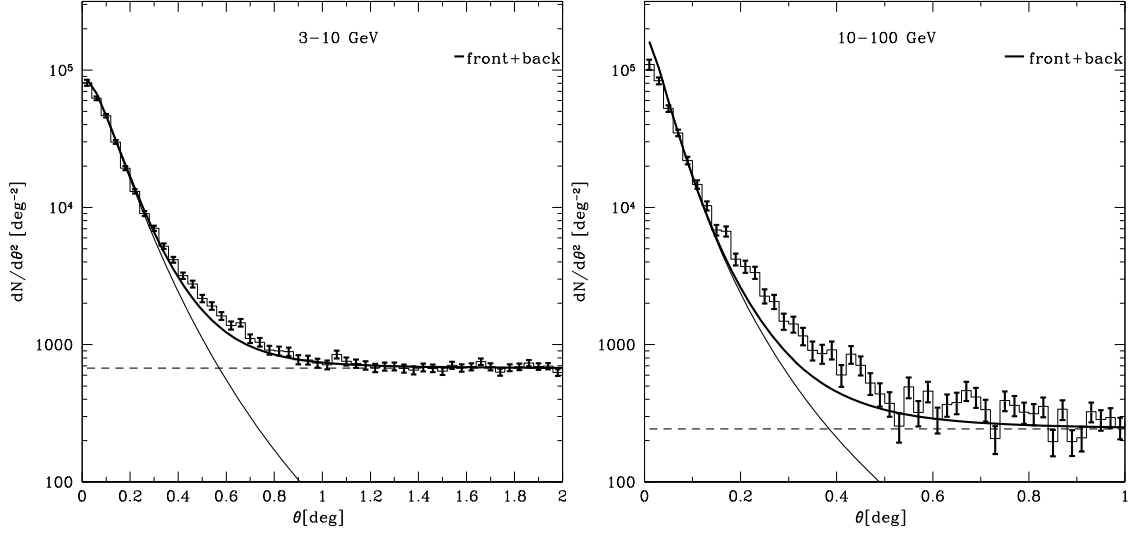


Fig. 2. Angular distribution of photons around stacked AGNs. Curves show the PSF (thin solid line), the background level (dashed line) and PSF plus background (thick solid line).

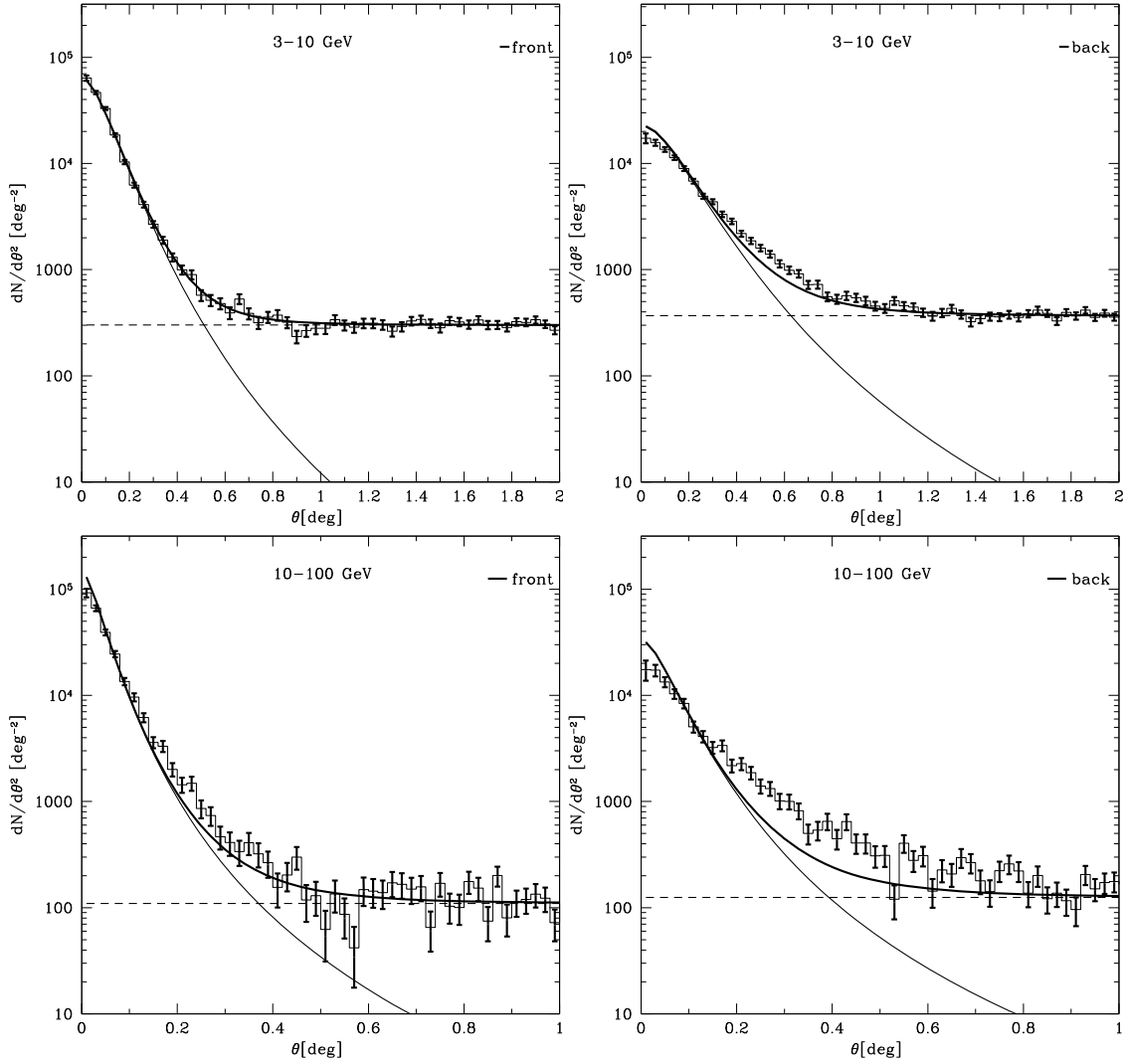


Fig. 3. The same as Fig. 2, but separately for the front (*left panel*) and back (*right panel*) photons in 3–10 GeV band (*top*) and 10–100 GeV band (*bottom*).

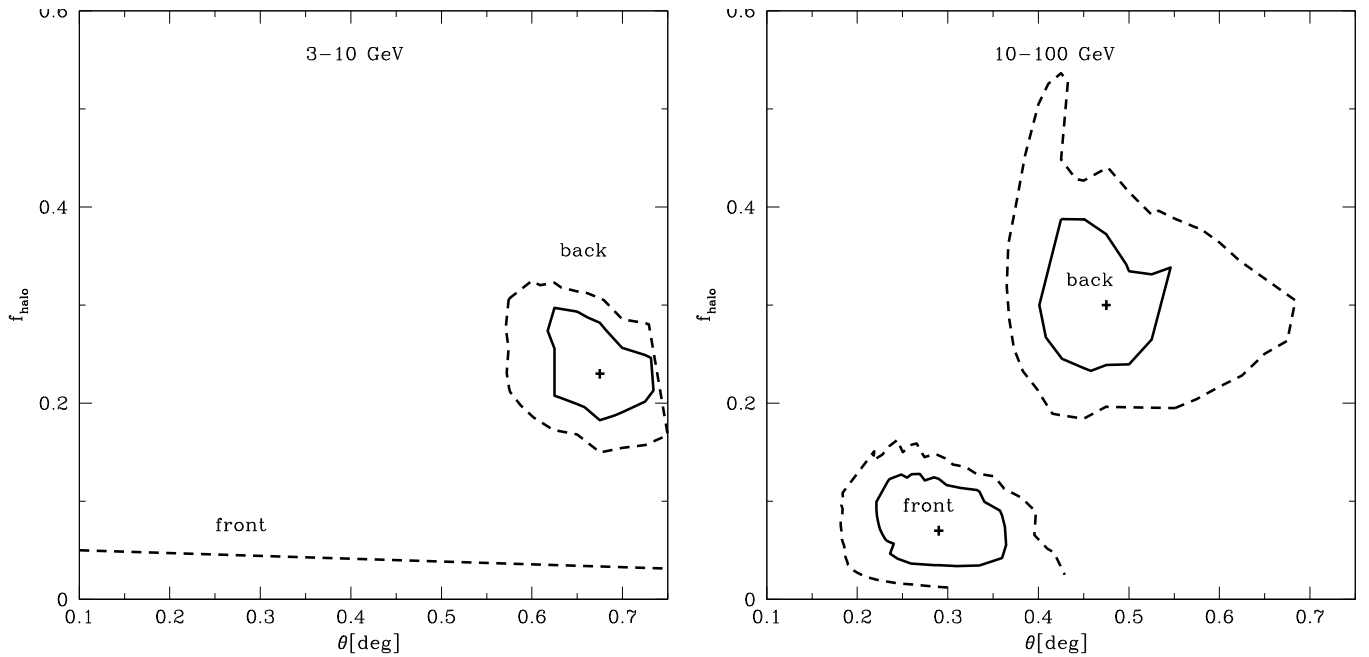


Fig. 4. 68% (solid) and 99% (dashed) confidence contours for the halo parameters θ_{halo} , f_{halo} derived from the separate analysis of front and back photons.

because in this case an equally strong excess should be detected in both the front and back photon signals.

To quantify the excess in the front and back photon signals above the DIFFUSE_P6_v3 PSF we followed Ando & Kusenko (2010) and introduced an additional θ^2 -Gaussian component $dN/d\theta^2 \sim \exp(-[\theta/\theta_{\text{halo}}]^4)$ in the model of the angular photon distribution. This additional component depends on two parameters, f_{halo} (fraction of the source signal contained in the additional component) and θ_{halo} (angular size of the core). Fitting the angular photon distributions with the improved model we found the best-fit values and confidence regions for f_{halo} , θ_{halo} separately for the front and back photons. The result is shown in Fig. 4. The parameters of the additional components found for the front and back photons are clearly different. An addition of the new component to the model does not improve the fit of the front photon angular distribution in the 3–10 GeV. Only an upper bound on the flux in the “halo” component could be derived, as is shown in the left panel of Fig. 4. This confirms our conclusion that the excess above the PSF is not caused by the real extended emission around AGN.

Indeed, the size and the flux of a real halo around AGN cannot depend on the way the photons were converted into e^+e^- pairs in the *Fermi*/LAT detector. Instead, the excess above the PSF in the back photons should be attributed to the imperfect modeling of the real PSF for back photons in the DIFFUSE_P6_v3 version of the LAT instrument characteristics.

To summarize, the angular distribution of photons around the stacked AGNs matches well that around the Crab source in both the 3–10 GeV and 10–100 GeV bands. A separate analysis of the front and back converted photons shows that there is no

evidence for a physical halo around AGN, neither in 3–10 GeV nor in 10–100 GeV band. No halo caused by the extragalactic magnetic fields is observed.

Acknowledgements. We thank A. Kusenko and S. Ando for the discussion of the subject. The work of PT is supported in part by IISN, Belgian Science Policy (under contract IAP V/27). The work of AN is supported by the Swiss National Science Foundation grant PP00P2_123426.

References

- Abdo, A. A., Ackermann, M., Ajello, M., et al. 2009, *Astropart. Phys.*, 32, 193
 Abdo, A. A., Ackermann, M., Ajello, M., et al. 2010, *ApJ*, 708, 1254
 Aharonian, F. A., Coppi, P. S., Volk, H. J. 1994, *ApJ*, 423, L5
 Ando, S., & Kusenko, A. 2010, *ApJ*, 722, L39
 Dolag, K., Kachelriess, M., Ostapchenko, S., & Tomas, R. 2009, *ApJ*, 703, 1078
 Dolag, K., Kachelriess, M., Ostapchenko, S., & Tomas, R. 2011, *ApJ*, 727, L4
 Elyiv, A., Neronov, A., & Semikoz, D. 2009, *Phys. Rev. D*, 80, 023010
 Franceschini, A., Rodighiero, G., & Vaccari, M. 2008, *A&A*, 487, 837
 Hester, J. J. 2008, *ARA&A*, 46, 127
 Kneiske, T. M., Bretz, T., Mannheim, K., & Hartmann, D. H. 2004, *A&A*, 413, 807
 Takahashi, K., Murase, K., Ichiki, K., Inoue, S., & Nagataki, S. 2008, *ApJ*, 687, L5
 Neronov, A., & Semikoz, D. V., 2007, *JETP Lett.*, 85, 473
 Neronov, A., & Semikoz, D. V. 2009, *Phys. Rev. D*, 80, 123012
 Neronov, A., & Vovk, Ie. 2010, *Science*, 328, 73
 Neronov, A., Semikoz, D. V., Kachelriess, M., Ostapchenko, S., & Elyiv, A. 2010, *ApJ*, 719, L130
 Plaga, R. 1995, *Nature*, 374, 430
 Stecker, F. W., & Scully, S. T. 2009, *ApJ*, 691, L91
 Tavecchio, F., Ghisellini, G., Foschini, L., et al. 2010, *MNRAS*, 406, L70
 Tavecchio, F., Ghisellini, G., Bonnoli, G., & Foschini, L. 2010, *MNRAS*, submitted [arXiv:1009.1048]